Human Molecular Genetics, 2011, Vol. 20, No. 2 **245–260**
doi:10.1093/hmg/ddq459
Advance Access published on October 20, 2010

A novel *Caenorhabditis elegans* allele, *smn-1(cb131)*, mimicking a mild form of spinal muscular atrophy, provides a convenient drug screening platform highlighting new and pre-approved compounds

James N. Sleigh[1], Steven D. Buckingham[1], Behrooz Esmaeili[1], Mohan Viswanathan[2,3], Edwin Cuppen[4], Bethany M. Westlund[2] and David B. Sattelle[1,5,*]

[1]MRC Functional Genomics Unit, Department of Physiology, Anatomy and Genetics, University of Oxford, South Parks Road, Oxford OX1 3QX, UK, [2]Cambria Pharmaceuticals, 14 Cambridge Center, Building 1, Cambridge, MA 02142, USA, [3]Department of Biology, Massachusetts Institute of Technology, Glenn Laboratory for the Science of Aging, 77 Massachusetts Avenue, Cambridge, MA 02139, USA, [4]Hubrecht Institute, KNAW and Department of Medical Genetics, University Medical Center Utrecht, Uppsalalaan 8, 3584 CT Utrecht, The Netherlands and [5]Faculty of Life Sciences, AV Hill Building, University of Manchester, Oxford Road, Manchester M13 9PT, UK

Received July 19, 2010; Revised September 30, 2010; Accepted October 11, 2010

Spinal muscular atrophy (SMA), an autosomal recessive genetic disorder, is characterized by the selective degeneration of lower motor neurons, leading to muscle atrophy and, in the most severe cases, paralysis and death. Deletions and point mutations cause reduced levels of the widely expressed survival motor neuron (SMN) protein, which has been implicated in a range of cellular processes. The mechanisms underlying disease pathogenesis are unclear, and there is no effective treatment. Several animal models have been developed to study SMN function including the nematode, *Caenorhabditis elegans*, in which a large deletion in the gene homologous to *SMN*, *smn-1*, results in neuromuscular dysfunction and larval lethality. Although useful, this null mutant, *smn-1(ok355)*, is not well suited to drug screening. We report the isolation and characterization of *smn-1(cb131)*, a novel allele encoding a substitution in a highly conserved residue of exon 2, resembling a point mutation found in a patient with type IIIb SMA. The *smn-1(cb131)* animals display milder yet similar defects when compared with the *smn-1* null mutant. Using an automated phenotyping system, mutants were shown to swim slower than wild-type animals. This phenotype was used to screen a library of 1040 chemical compounds for drugs that ameliorate the defect, highlighting six for subsequent testing. 4-aminopyridine, gaboxadol hydrochloride and *N*-acetylneuraminic acid all rescued at least one aspect of *smn-1* phenotypic dysfunction. These findings may assist in accelerating the development of drugs for the treatment of SMA.

INTRODUCTION

Spinal muscular atrophy (SMA), an autosomal recessive neurodegenerative disease, is one of the principal genetic causes of infant death and is characterized by targeted loss of lower motor neurons, leading to muscular wasting and paralysis (1,2). SMA results from diminished expression/function of the widely expressed survival motor neuron (SMN) protein (3), which has been implicated in a number of cellular processes including small nuclear ribonucleoprotein (snRNP)

*To whom correspondence should be addressed at: Faculty of Life Sciences, AV Hill Building, University of Manchester, Oxford Road, Manchester M13 9PT, UK. Tel: +44 1612755408; Fax: +44 1612755948; Email: david.sattelle@manchester.ac.uk

assembly, pre-mRNA splicing, axonal transport, transcription and small nucleolar RNP biogenesis (4–9). Humans possess two genes encoding SMN: a telomeric copy (*SMN1*) and a centromeric copy (*SMN2*) (3). *SMN1*, the SMA-determining gene, encodes a full-length, functional protein, whereas *SMN2* contains a translationally silent C-to-T mutation within exon 7, causing most *SMN2* transcripts to be alternatively spliced and the resulting protein to be rapidly degraded (10). *SMN2* copy number often inversely correlates with SMA severity, so *SMN2* is thought to act as a disease modifier when *SMN1* is dysfunctional (11,12).

Currently, there are no effective treatments for SMA. Of the various compounds that have been explored as potential therapies (13–19), even the most promising, including phenylbutyrate and valproic acid, have negligible and/or short-lived benefits sometimes with undesirable side effects (20–24). The approach of screening libraries containing drugs approved for human use has successfully highlighted potential pharmacological agents for the treatment of several neurodegenerative disorders including amyotrophic lateral sclerosis and Huntington's disease (25,26). Interestingly, a number of drugs used to treat various other diseases have shown off-label effects that may prove beneficial to SMA sufferers (27,28). Thus, screening pre-approved compounds for potential as SMA therapeutics may accelerate the identification and development of drugs helpful in treating the disease.

For speed and economy of testing, invertebrate organisms offer convenient models for chemical screening (29,30). The nematode *Caenorhabditis elegans* is ideal in this regard, with added benefits of fast generation time, substantial reproductive capacity, ease of large-scale culture and potential for automated behavioral analysis (31,32). *C. elegans* can be quickly dispensed into 96-well plates containing chemical compounds and screened for alteration of easily scorable phenotypes. Several drugs currently used in the clinic to treat neurodegenerative diseases are also efficacious in *C. elegans* models (33–35). This small invertebrate is thus a powerful tool with which to triage compounds from large chemical libraries prior to validation in vertebrate models. Indeed, a *C. elegans* model of Duchenne muscular dystrophy was recently used to screen and identify compounds that caused improvement of muscle strength in the dystrophic mouse model (36).

C. elegans possesses a single gene (*smn-1*) homologous to *SMN*, which is expressed throughout development and in a number of cell types including neurons and body wall muscles (37). Like human SMN, SMN-1 has been shown to self-oligomerize and bind to the *C. elegans* homolog of human Gemin2 (37,38). Disruption of endogenous SMN-1 function using RNA interference (RNAi) results in various phenotypic defects including locomotor dysfunction and sterility (37), and a null mutant, *smn-1(ok355)*, displays a range of morphological and physiological defects including abnormal germline migration and severely reduced swimming (thrashing) rate (39). This model was used to show that neuronal- but not muscle-directed expression of SMN-1 could partially rescue the phenotype, although the mutants remained sterile (39). The *smn-1(ok355)* mutant animals appear normal during early development due to maternal loading of SMN-1 protein and mRNA, but rapidly deteriorate in later larval stages (39). The *smn-1(ok355)* deletion is homozygous lethal and so must be maintained using a chromosomal balancer, limiting the ease with which the mutant can be used for large-scale screening. Nevertheless, a genome-wide RNAi screen using this model recently identified endocytosis and mRNA regulation pathways as being critical *smn-1* modifiers (40).

Here, we have isolated and characterized a new allele, *smn-1(cb131)*, that encodes an amino acid substitution closely resembling a change in SMN found in a patient with the less severe, yet still debilitating, type IIIb form of SMA (41). This alteration in human SMN affects N-terminal self-association, Gemin2 binding, snRNP assembly activity and protein stability *in vitro* (42). The homozygous *smn-1(cb131)* mutant displays milder phenotypic defects than the null mutant and is fertile, obviating the need for a balancer chromosome. We screened a library of 1040 diverse compounds, including many with known human therapeutic profiles and nerve/muscle activity, for amelioration of the *smn-1(cb131)* thrashing defect with the goal of expediting the development of drugs for the treatment of SMA.

RESULTS

The reduced growth and lifespan of the *smn-1(cb131)* allele

C. elegans possesses a single gene (*smn*-1) homologous to human *SMN,* which is widely expressed throughout embryonic development and into adulthood (37). *smn-1(cb131)* (strain LL2073), isolated in a reverse genetic screen for *smn-1* mutants, contains a novel point mutation in exon 2 that alters a highly conserved amino acid residue (D27N) in the SMN-1 protein (Fig. 1). This same residue (D44V) is mutated in a patient with type IIIb SMA (41).

There does not appear to be any gross change in the rate of development of *smn-1(cb131)* compared with wild-type up to 4 days post the larval L1 stage (Fig. 2). The developmental stage of mutant and wild-type animals was scored 24, 48 and 72 h after eggs were laid, and no difference between strains was seen at any time point (data not shown). However, 3–5 days post-L1, the mutant body length was significantly shorter than that of the wild-type, with the growth of *smn-1(cb131)* animals appearing to cease between 2 and 3 days post-L1 whereas wild-type continued to grow (Fig. 3A). The median and mean values of the *smn-1(cb131)* body length were within 11 μm of each other on days 3–5. *smn-1(cb131)* also displayed a significantly reduced lifespan with median survival at 15 days compared with 17 days for wild-type at 23.5°C (Fig. 3B). During lifespan assays, mutant animals stopped moving around the plate sooner than wild-type, indicating an accelerated age-associated decline in movement.

Defects in egg-laying and hatching

On food, age-synchronized young adult *smn-1(cb131)* animals laid approximately half as many eggs as wild-type (Fig. 4A). Since food cues play an important role in egg-laying behavior (43), the response of *smn-1(cb131)* to the absence of food was also assessed. As expected, wild-type animals laid

Figure 1. *smn-1(cb131)* harbors a novel point mutation that mimics a substitution seen in a SMA type IIIb patient. In *C. elegans* SMN-1 (CeSMN-1), aspartic acid (D) at residue 27 is mutated to asparagine (N). In human SMN (hSMN), D is mutated to valine (V) at residue 44.

considerably fewer eggs without food. The *smn-1(cb131)* animals also laid significantly fewer eggs, suggesting that the egg-laying defect was not a result of a deficit in food chemosensation or sensory processing of food cues.

There was also no difference in the number of eggs retained in the uterus of mutant and wild-type animals (Fig. 4B), which was confirmed by sodium hypochlorite bleaching of the cuticle and counting of the number of released eggs (data not shown). Due to increased egg retention, egg-laying defective mutants usually bloat and show an enhanced tendency for internal hatching of larvae (44), but this was not common in *smn-1(cb131)*, which could mean that the defect is perhaps pre-egg-laying, i.e. in the generation of embryos, maybe due to a sperm and/or oocyte defect. Brood size assays confirmed that egg production is affected; *smn-1(cb131)* animals laid fewer eggs over a lifetime than wild-type (Fig. 4C). During the retention assay, there was an indication that some mutant uteri were less well organized than in wild-type, with less distinct egg boundaries. Also, some mutant animals expelled an amorphous substance from the vulva into the medium. On plates, ~5–10% of the eggs laid were unusually circular, discolored and/or large. Eggs laid by *smn-1(cb131)* mutants hatched at a slightly lower frequency than those laid by wild-type (Fig. 4D).

Pharyngeal pumping rate is unaffected but motility is defective

The *C. elegans* pharynx, a neuromuscular pump used to ingest and break up food, pumps back and forth in an easily quantifiable manner. Similarly, when placed in liquid, *C. elegans* swim (thrash) back and forth at a regular rate. Pharyngeal pumping and thrashing assays are thus simple, robust methods for assessing neuromuscular function. *smn-1(ok355)* null mutants (strain LM99) show a dramatic and progressive decline in pharyngeal pumping and thrashing rates at the L2/L3 stage that continues until death a few days later (39).

To assay pharyngeal pumping rates of *smn-1(cb131)*, animals were filmed for a period of 10 s, and videos were played back in slow motion to enable accurate counting. Mutant pumping rates were indistinguishable from wild-type prior to day 10 post-L1, but differed significantly on day 10, suggestive of an enhanced age-related degeneration of pharyngeal function (Fig. 5A).

Thrashing assays were performed in phosphate-buffered saline (PBS) on 1–5 consecutive days post-L1. Similar to wild-type, *smn-1(cb131)* animals showed a gradual reduction in thrashing rate over time; however, no striking decline was noted as seen in the null mutant (Fig. 5B). Nevertheless, *smn-1(cb131)* did consistently thrash at a significantly reduced rate compared with wild-type animals at all times tested, indicating a robust motility defect.

Synaptic neurotransmission is deficient in *smn-1(cb131)* animals

In order to determine a potential origin for the motility defect, muscle and nervous system architecture in young adults were examined. The musculature of wild-type and *smn-1(cb131)* animals was assessed by Nomarski microscopy (Fig. 6A and B) and by fluorescence microscopy of phalloidin F-actin staining (Fig. 6C and D); no obvious differences in muscle size, structure or orientation were seen, suggesting that the motility defect of *smn-1(cb131)* is unlikely to be due to muscle structure degradation. To perform neuron counts and to observe the morphology of the nervous system, *smn-1(cb131)* animals were crossed with a strain expressing pan-neuronal green fluorescent protein (GFP), *F25B3.3::GFP* (45), to produce *smn-1(cb131); F25B3.3::GFP* (strain LM123), confirmed by sequencing. Using White *et al.* (46) as a guide, GFP-positive neuron cell bodies in the ventral nerve cord, which includes cholinergic and gamma-aminobutyric acid (GABA)-ergic neurons that control locomotion, were counted (Fig. 6E). No difference was seen between *smn-1(cb131)* and control animals, a result similar to that seen for the null mutant (39). The nervous systems of the two strains were then examined in more detail for subtle abnormalities that may account for the motility defect. The organization of both the ventral and the dorsal nerve cords was inspected, as well as neuronal trajectories, but no obvious differences in morphology were seen.

Since the structure of the neuromuscular system was not grossly affected, synaptic transmission efficiency of *smn-1(cb131)* was assessed using the acetylcholinesterase inhibitor, pyridostigmine bromide. Pyridostigmine bromide disrupts the enzymatic breakdown of acetylcholine and its subsequent clearance from the synaptic cleft, causing neurotransmitter accumulation and thus muscle hypercontraction. It has been used for many years to treat post-synaptic myasthenic disorders (47) and for this reason was chosen for paralysis assays. The time taken for *C. elegans* to paralyze in the presence of the drug gives an indication of whether synaptic neurotransmission at the neuromuscular junction is altered. The mutant appears to be relatively resistant to the drug (Fig. 6F), suggesting that synaptic transmission is defective in *smn-1(cb131)* animals.

smn-1(cb131) defects are specific to the point mutation

To confirm that *smn-1(cb131)* is indeed an allele of *smn-1* and that defects seen in the strain are due to the mutation in *smn-1*, a complementation test was performed (48). *smn-1(cb131)* was combined *in trans* with *smn-1(ok355)* by crossing *smn-1(cb131)* males with *smn-1(ok355)/hT2*[*qIs48*] hermaphrodites, producing *smn-1(cb131) smn-1(ok355)* (strain LM124) progeny. The thrashing rate of these animals was significantly slower than that of wild-type and homozygous *smn-1(cb131)* animals at the young adult stage (Fig. 7). This suggests that the product of neither allele restores wild-type

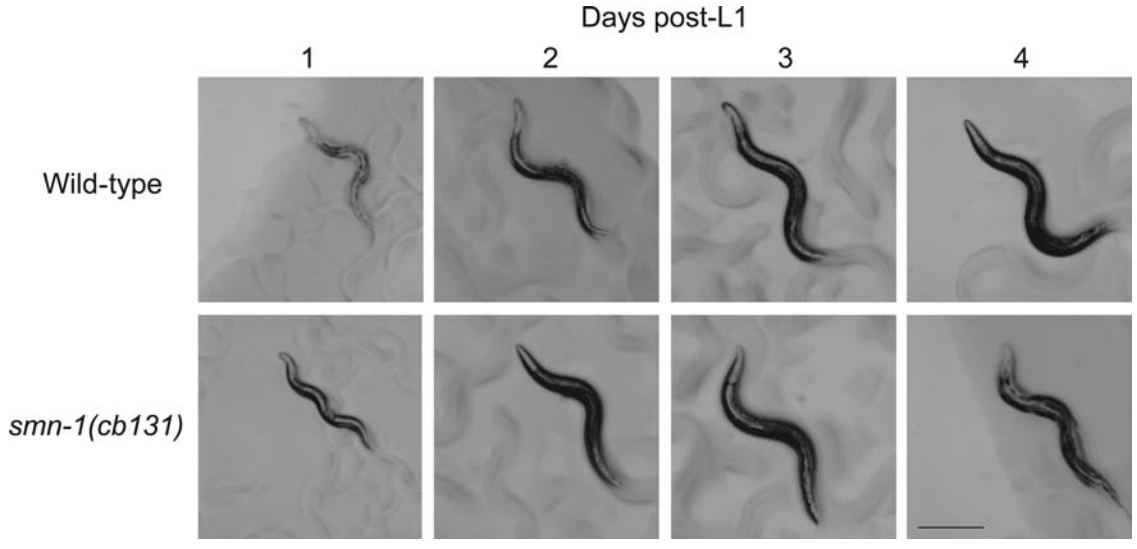

Figure 2. Developmental comparison of *smn-1(cb131)* with wild-type. There is no obvious developmental difference between *smn-1(cb131)* and wild-type. The strain is indicated on the left and the number of days post-L1 of the age-synchronized animals above. For all images, the head is on the left and the tail on the right. Scale bar = 400 μm.

function, meaning that they do not complement and are therefore likely to be alleles of the same gene. However, for complementation testing to work, both alleles must be recessive. *smn-1(ok355)* is recessive as it is a deletion. To provide evidence that *smn-1(cb131)* is recessive, *smn-1(ok355)/hT2*[*qIs48*] and *smn-1(cb131)/hT2*[*qIs48*] (strain LM125) animals were also assayed for thrashing (Fig. 7). If *cb131* were a dominant mutation, the thrashing rate of *smn-1(cb131)/hT2*[*qIs48*] animals would be expected to be similar to *smn-1(cb131)*, because of the presence of the mutated allele, and less than *smn-1(ok355)/hT2*[*qIs48*], because of the absence of *cb131*. However, this was not the case, suggesting that *cb131* is recessive. *smn-1(cb131)/hT2*[*qIs48*] animals were allowed to lay eggs before assaying so as to be able to subsequently differentiate them from any self-progeny of *smn-1(ok355)/hT2*[*qIs48*] hermaphrodites, which produce *smn-1(ok355)* null mutants.

Evaluating an automated *smn-1(cb131)* swimming (thrashing) assay

To determine whether the *smn-1(cb131)* thrashing defect could be used as the basis of an *in vivo*, automated chemical library screen, thrashing rates of wild-type and *smn-1(cb131)* animals were measured using an automated phenotyping system, developed for measuring the effects of chemicals on locomotion (32). Synchronized young adults (2 days post-L1) were assayed at various time points in liquid suspension from 10 min to 6 h. Young adults were used because thrashing rates of larval stage animals cannot be accurately determined with the automated software, and assaying a day later would allow sufficient time for progeny of the age-synchronized nematodes to reach a size that confounds quantification of thrashing of the parent generation. Similar to the results of the manual assay, the automated assay was able to detect a significant difference between wild-type and *smn-1(cb131)* animals; the mutants consistently thrashed at a slower rate at all time points in solution (Fig. 8).

Screening of a chemical library identifies six compounds

The National Institute of Neurological Disorders and Stroke (NINDS) chemical compound library was used to screen *smn-1(cb131)* animals for amelioration of the motility defect. The library consists of 1040 compounds covering a wide range of drug classes (listed at http://www.msdiscovery.com/ last accessed October 19, 2010), the majority of which are approved for use in humans by the US Food and Drug Administration (FDA) (49–51). An overview of the entire screening process can be seen in Figure 9A. In brief, for the primary screen, 2–25 age-synchronized *smn-1(cb131)* young adult animals were dispensed into each well of 96-well plates containing library compounds dissolved in dimethyl sulfoxide (DMSO) at 1 mM (10 μM compound and 1% DMSO after addition of liquid and nematodes). Thrashing rates were measured using the previously described automated phenotyping system 4 and 6 h after addition of the animals (32). The top 64 compounds (Fig. 9B) that increased thrashing rate at both time points included 48 pre-approved compounds and comprised various receptor agonists (e.g. cholinergic, GABAergic, glutamatergic and serotonergic) and muscle relaxants (both skeletal and smooth). These 64 compounds were re-tested in triplicate on both wild-type and *smn-1(cb131)* animals in dose–response format at concentrations ranging from <0.1 to 50 μM in order to highlight the most promising for further study. Six compounds, including four pre-approved drugs, were selected based on dose-dependence, a non-linear regression coefficient (R^2) > 0.1 and a point along the line of regression ≥ 7.3 at both 4 and 6 h. The six compounds were aklavin hydrochloride, 4-aminopyridine (4-AP), gaboxadol hydrochloride, metaraminol bitartrate, *N*-acetylneuraminic acid (Neu5Ac) and zidovudine.

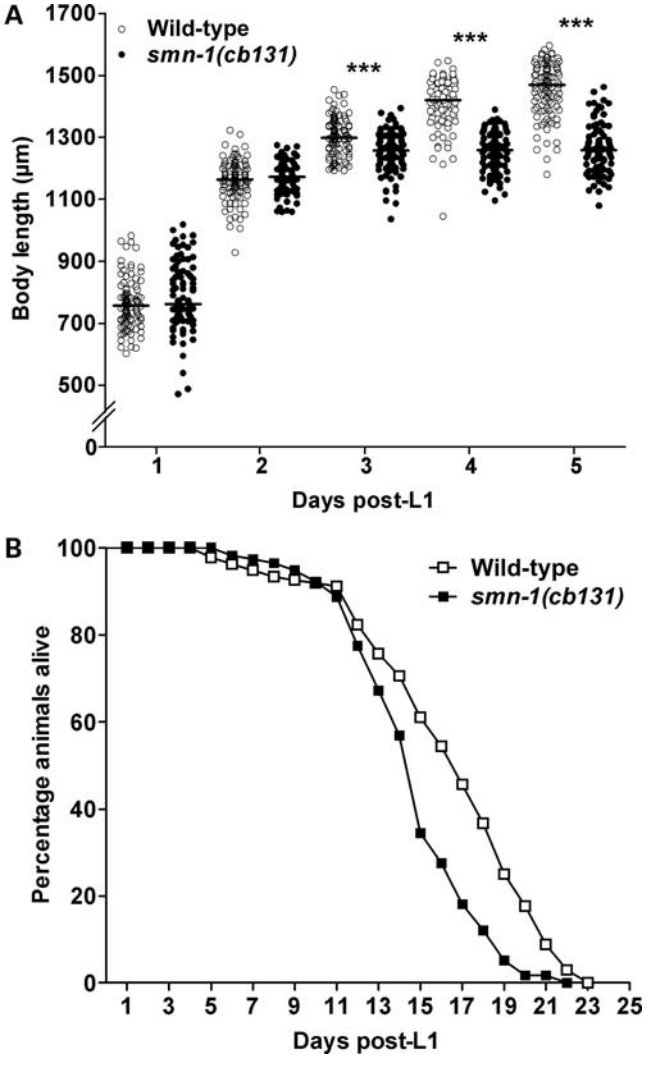

Figure 3. Body length and survival measurements of wild-type and *smn-1(cb131)*. (**A**) *smn-1(cb131)* grows at a rate similar to wild-type up to 2 days post-L1; however, after 3, 4 and 5 days, they have a significantly shorter body length. The *smn-1(cb131)* animals were 95.9 ± 1.6, 88.7 ± 0.6 and 87.0 ± 0.6% the length of wild-type animals on days 3, 4 and 5, respectively. Individual measurements are plotted and lines indicate the median values. One hundred animals per strain per time point were assayed. ***$P <$ 0.001, Mann–Whitney *U* test. (**B**) *smn-1(cb131)* ($n = 115$) has a median survival of 15 days and wild-type ($n = 136$) 17 days at 23.5°C. $P < 0.001$, log-rank (Mantel–Cox) test; $P < 0.001$, Gehan–Breslow–Wilcoxon test. Data points represent the percentage of age-synchronized animals found alive each day post-synchronization. Data from three independent assays are presented. In each experiment, wild-type animals lived longer than mutant with $P < 0.001$, $P = 0.002$ and $P = 0.119$, log-rank (Mantel–Cox) test.

Validation of the top 6 compounds

In order to identify which, if any, of the six compounds could robustly and significantly improve motility of *smn-1(cb131)*, additional thrashing assays were performed. The most effective concentration for each compound from the dose–response assays was used. This was 25 μM for 4-AP, gaboxadol hydrochloride and Neu5Ac, 12.5 μM for metaraminol bitartrate and 6.25 μM for zidovudine. Unfortunately, aklavin hydrochloride was unavailable. Compounds used in these assays were purchased from a source independent of the NINDS library manufacturer. Age-synchronized young adults were assayed in the presence of drugs at 1.5, 2, 2.5 and 3 h (Fig. 10A). 4-AP significantly improved *smn-1(cb131)* motility at all time points and had no effect on wild-type. However, it also increased the thrashing frequency of *unc-63(x26)* (strain ZZ26) after 1.5–2.5 h, which was included to test the specificity of the drugs for the *smn-1(cb131)* mutation. Impaired expression of *unc-63*, a nicotinic acetylcholine receptor subunit found in both muscles and neurons, results in locomotor dysfunction (52–54). *unc-63(x26)* was thus included as a control because it encodes a point mutation in *unc-63*, which is important for synaptic transmission (52), that results in a mild motility defect (54).

The top 5 available compounds were also tested for their ability to improve the *smn-1(cb131)* egg-laying defect. In brief, L4 stage animals were transferred to new plates containing compounds at 50 μM and left to mature overnight. Eggs from these age-synchronized animals were then transferred to new drug plates, placed at 23.5°C for 72 ± 1 h, and the number of eggs laid by young adults in 2 h was assessed. Drugs were also added at the same final concentration to the food used to seed the plates; only zidovudine was seen to affect the growth of the bacterial lawn, causing small distinct clusters of food to form and the lawn to take on a slightly darker appearance. No compound significantly affected wild-type egg-laying (Fig. 10B); however, Neu5Ac significantly increased the number of eggs laid by *smn-1(cb131)* by 26.1 ± 6.0%. Gaboxadol hydrochloride also appeared to improve egg-laying, albeit not reaching significance.

Efficacy of compounds in the *smn-1* null mutant

The top 5 compounds were tested for their ability to rescue lifespan, body length and pharyngeal pumping, all of which are severely reduced, in the null mutant, *smn-1(ok355)* (39). Animals heterozygous for the balancer chromosome and the *smn-1* deletion that were raised from hatching on 50 μM drug plates were allowed to lay eggs for 5 h on new drug plates and removed. The homozygous *smn-1* progeny were then assayed for survival each day until death and for body length and pumping at various time points. No compound significantly affected *smn-1(ok355)* longevity, although zidovudine did extend the median lifespan of control from 6 to 7 days, which approached significance (data not shown). In the body length assays, no compound had a significant effect 1–2 days post-L1; however, after 3 days, both 4-AP and gaboxadol hydrochloride caused significant rescue (Fig. 11A). 4-AP also significantly improved pharyngeal pumping rate of the *smn-1* null mutant 3 and 4 days post-L1, whereas Neu5Ac significantly improved pumping on day 4 (Fig. 11B).

DISCUSSION

SMA is a debilitating neuromuscular disease caused by attenuated function of the SMN protein. Despite being one of the primary genetic causes of infant mortality, there is currently no effective treatment. Various compounds enhance SMN expression *in cellulo* by up-regulating *SMN2* transcription or

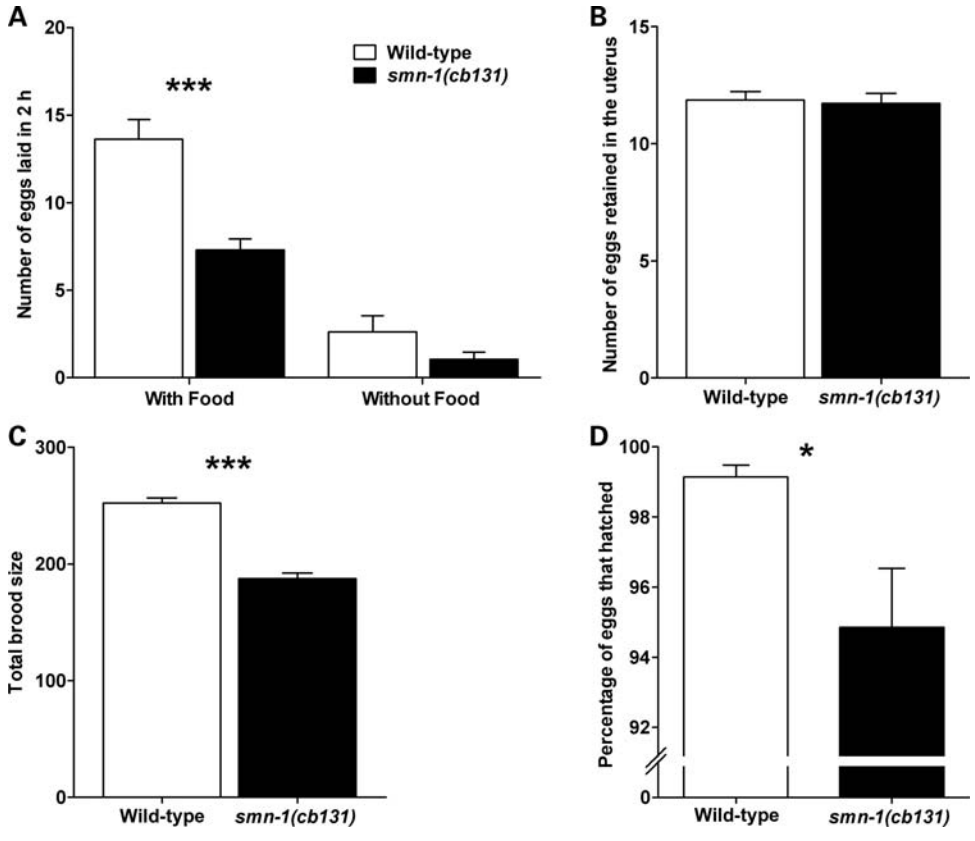

Figure 4. Characterization of *smn-1(cb131)* egg-laying behaviors. (**A**) In 2 h at 23.5°C, age-synchronized young adult *smn-1(cb131)* animals laid approximately half the number of eggs as wild-type on food. However, they responded normally to food cues, laying significantly fewer eggs without food. About 23–24 animals were assayed per strain for each condition over three independent experiments. $^{***}P < 0.001$, unpaired *t*-test with Welch's correction. (**B**) There was no difference in the number of eggs retained in the uterus of wild-type and *smn-1(cb131)* young adults. Thirty animals were assayed per strain over three independent experiments. An unpaired *t*-test was used to test for significance. (**C**) The total brood size of *smn-1(cb131)* animals was reduced. Thirty animals were assayed per strain over three independent experiments. $^{***}P < 0.001$, unpaired *t*-test with Welch's correction. (**D**) The percentage of mutant eggs laid by young adults that failed to hatch is six times that of wild-type (5.14 and 0.86%, respectively). Hatching percentages were calculated for individual sets of at least 50 eggs. About 650 eggs were assayed per strain over seven independent experiments. $^{*}P < 0.05$, unpaired *t*-test with Welch's correction. Means ± SEM are plotted for all figures.

by increasing the number of *SMN2* transcripts containing exon 7 (55–58); however, limitations of toxicity and/or rapid metabolism often restrict their utility. A novel *C. elegans smn-1* mutant, *smn-1(cb131)*, with a point mutation in a highly conserved residue of exon 2 (Fig. 1), was used to screen a library of 1040 compounds using an automated system capable of determining *C. elegans* swimming (thrashing) frequencies. To our knowledge, this is the first chemical compound screen performed on an *in vivo* model of SMA and, as such, will be informative in future studies to explore the therapeutic potential of these compounds and their analogs for the treatment of SMA.

smn-1(cb131) is a non-lethal mutant, well suited to screening

Reduction of SMN-1 expression in *C. elegans* by means of RNAi causes a multitude of defects, including reduced motility, severely diminished fertility and, ultimately, larval lethality, suggesting that SMN-1 is essential in *C. elegans* as in humans (37). Recently, a null mutant, *smn-1(ok355)*, was generated, which shows comparable defects (39). The homozygous null displays larval lethality, arresting at the L2/L3 stage, and a rapid degeneration of motility and neuromuscular function, thought to coincide with the depletion of maternally loaded SMN-1 protein and mRNA (39). Since *smn-1(ok355)* is homozygous lethal and must be maintained using a balancer chromosome, this allele is technically demanding for screening on a large scale. Unlike *smn-1(ok355)*, *smn-1(cb131)* is a milder allele of *smn-1* that is fertile and produces progeny that reach adulthood. Since all animals are homozygous for the mutation, there is no requirement for elaborate or costly equipment to isolate large numbers of a particular genotype (59). *smn-1(cb131)* mutant animals display readily quantifiable defects including diminished body length (Fig. 3A), lifespan (Fig. 3B), egg-laying (Fig. 4) and, in particular, motility (Fig. 5B), which are specific to the point mutation in *smn-1* (Fig. 7); however, these defects are much less severe than in *smn-1(ok355)* and therefore enable the study of SMN-1 function into adulthood.

Animals bearing the *smn-1 cb131* mutation lay significantly fewer eggs (Fig. 4A). This defect is unlikely to be caused by a deficiency in chemosensation as fewer eggs were laid in the

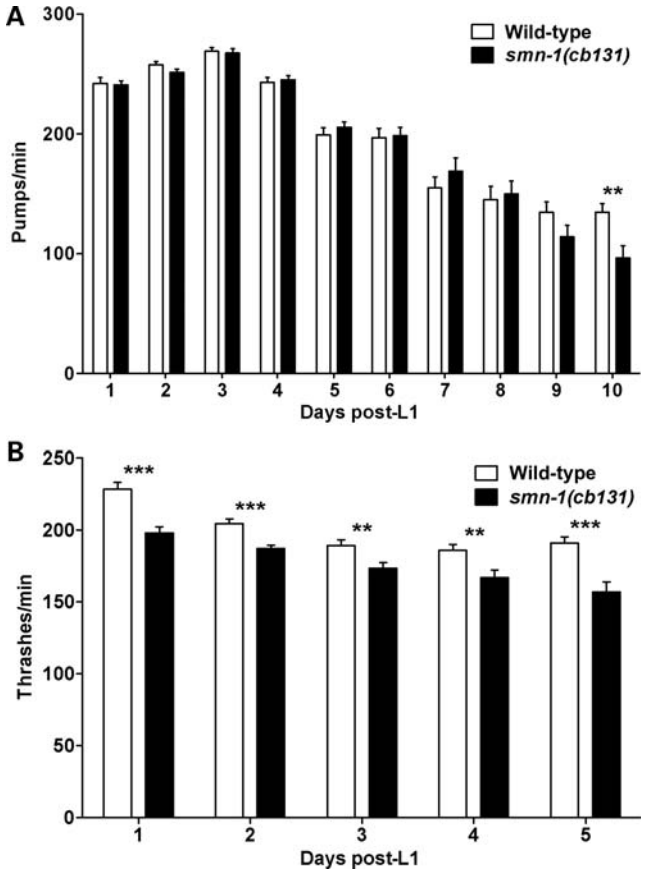

Figure 5. *smn-1(cb131)* pharyngeal pumping and thrashing rates. (**A**) Pharyngeal pumping rates of wild-type and *smn-1(cb131)* 1–10 days after larval L1 stage. *smn-1(cb131)* pumping rates are indistinguishable from wild-type at all time points excluding day 10. At least 24 animals per strain per time point were assayed over three independent experiments. $^{**}P < 0.01$, unpaired *t*-test. (**B**) Thrashing rates of wild-type and *smn-1(cb131)* after 10 min in PBS 1–5 days post larval L1 stage counted manually. *smn-1(cb131)* consistently thrashes at a slower rate than age-synchronized wild-type. The *smn-1(cb131)* animals thrashed at 86.8 ± 5.0, 93.1 ± 5.4, 91.6 ± 5.2, 90.0 ± 8.5 and 82.9 ± 3.0% of the rate of wild-type on days 1–5, respectively. At least 22 animals per strain per time point were assayed over three independent experiments. $^{**}P < 0.01$ and $^{***}P < 0.001$, Mann–Whitney *U* test or unpaired *t*-test with Welch's correction. Means ± SEM are plotted for both figures.

absence of food, as seen in wild-type animals. Usually, egg-laying defective mutants lay fewer eggs and consequently retain more in the uterus (44); however, this was not observed in *smn-1(cb131)* animals, which behaved similarly to wild-type in this regard (Fig. 4B). This, coupled with observations of minor germline disorganization, an increased percentage of embryonic lethality and reduced total brood sizes (Fig. 4C and D), suggests that the *cb131* mutation reduces egg viability and decreases fertility. This situation is mirrored by *smn-1* RNAi, in which syncitial germ cells very quickly fail to proliferate and differentiate before the somatic gonad and behavioral phenotypes are affected, indicating that the germline is perhaps among the most susceptible tissues to SMN mutation (37).

Unlike the null mutant, *smn-1(cb131)* does not display a rapidly progressive decline in neuromuscular function. Interestingly, thrashing, but not the pharyngeal pumping ability of *smn-1(cb131)*, is defective, suggesting that these tissues are differentially affected by the *cb131* mutation. This may reflect a disparity in the requirements of SMN-1 in different muscle types. There are striking biochemical (60,61) and physiological (62) differences between body wall and pharyngeal muscles. In particular, *C. elegans* pharyngeal muscle is capable of myogenic activity; the pharynx continues pumping despite laser ablation of the entire nervous system innervating the structure, similar to cardiac myocytes (62). These differences may underlie the disparate susceptibility to altered SMN-1 function. Since the frequency of pharyngeal pumping is unaffected in *smn-1(cb131)* animals, it is unlikely that the observable phenotypic defects are caused by lack of food. This is supported by the observation that *cb131* adults do not display the paler, starved appearance seen in the *ok355* null mutant animals (39). A similar differential susceptibility to SMN loss by different muscle types has been reported in two different mouse models of SMA; neuromuscular pathology appears sooner in a predominantly slow-twitch postural muscle compared with two exclusively fast-twitch muscles found in the trunk and lower limbs (63). Neurotransmitter release in the postural muscle has also been shown to become impaired before neurotransmission in the trunk muscle, corroborating the morphological findings (64). Selective muscle type vulnerability is a SMA disease hallmark, as it is characterized by proximal muscle weakness, with certain muscles such as the diaphragm appearing relatively unaffected (65).

To find an explanation for the motility defect of *smn-1(cb131)*, body wall musculature and nervous system morphology were observed (Fig. 6A–E); no gross structural defects in either tissue were seen. Synaptic function was thus explored using the acetylcholinesterase inhibitor, pyridostigmine bromide (Fig. 6F). The *smn-1(cb131)* animals took longer to paralyze on plates containing the drug, suggesting that synaptic transmission between cholinergic ventral nerve cord motor neurons and body wall muscles is disrupted (66,67), a phenomenon seen in *Drosophila* (68) and mouse models of SMA (64,69). Given that the ventral nerve cord neuron number is unchanged and that muscle structure appears unaffected, this deficiency at the synapse may be the principal cause of the motility defect. Interestingly, mutations that affect cholinergic neurotransmission have also been shown to result in the impairment of egg-laying (70), which is a phenotype seen in *smn-1(cb131)* animals (Fig. 4A). Furthermore, two *C. elegans* neuronal, RNA-binding splicing factors that localize to the nucleus, UNC-75 and EXC-7, have also been implicated in synaptic transmission, providing a link between RNA processing and synaptic transmission (71), which may be particularly relevant to SMA.

Chemical screening using *C. elegans*

The NINDS library consists of 1040 chemicals from a range of drug classes, the majority of which have known targets and are approved for use in humans by the FDA (49–51). If such a compound should be found to be efficacious for the treatment of a disease, it may furnish a faster route from the laboratory to the clinic. The ease with which large collections of drugs can be screened, coupled with the speed and low cost of using

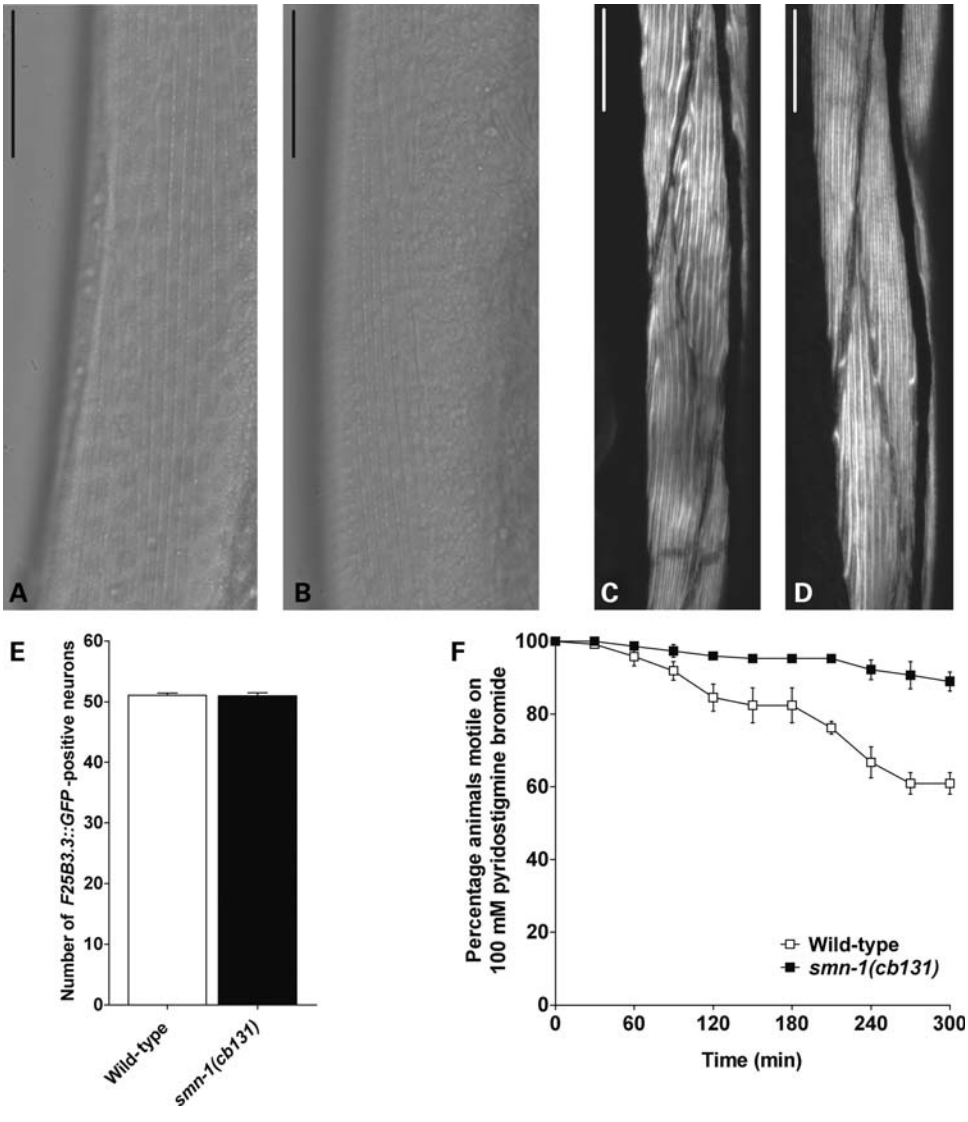

Figure 6. The *smn-1(cb131)* animals have no gross structural defects in muscles or neurons, but display impaired synaptic transmission. (**A** and **B**) Nomarski and (**C** and **D**) fluorescence microscopy of phalloidin staining of wild-type (A and C) and *smn-1(cb131)* (B and D) muscle structure. *smn-1(cb131)* muscle size, structure and orientation are all similar to wild-type. For all images, the head is situated upwards and images are taken of regions anterior to the vulva. Scale bars = 25 μM. (**E**) *smn-1(cb131)* animals display no reduction in the number of neuron cell bodies in the ventral nerve cord. GFP-positive cells expressing the pan-neuronal marker *F25B3.3::GFP* were counted from and including VA2 (anterior) to VD11 (posterior). Thirty young adults were assayed per strain over three independent experiments. An unpaired *t*-test was used to test for significance. Means ± SEM are plotted. (**F**) *smn-1(cb131)* animals are resistant to the acetylcholinesterase inhibitor pyridostigmine bromide. Data points represent the mean ± SEM percentage of age-synchronized young adults found moving on 100 mM plates at 30 min intervals over a period of 6 h. $P < 0.001$, log-rank (Mantel–Cox) test; $P < 0.001$, Gehan–Breslow–Wilcoxon test. Data from three independent assays are presented $P = 0.0011$, $P = 0.128$ and $P = 0.0026$, log-rank (Mantel–Cox) test.

C. elegans, provides a very efficient combination for highlighting compounds with therapeutic potential (30). Vital to this utility for drug screening, ∼60% of the human genes have a *C. elegans* homolog, suggesting that many biochemical pathways are conserved and that compounds affecting *C. elegans* may also lead to the rapid translation toward the clinic of lead compounds for the treatment of human disease (72,73). It is not feasible to perform large-scale screens on mouse models of disease, so invertebrates such as *C. elegans* offer a first-pass filter to identify putative novel targets and drug leads *in vivo*. In addition, screening drugs in live models can also help to eliminate compounds with systemic toxic properties. The development of a high-throughput, whole-animal chemical screen on a genetic model of SMA is likely to be more powerful and advantageous than a screen only focussed on identifying compounds with specific effects of increasing SMN expression levels, in that it may identify drugs that target pathways not directly related to SMN, thus highlighting novel potential pharmacological agents. This aspect of whole-animal, *in vivo* screening is particularly useful for diseases such as SMA, in which the pathophysiology is not yet fully established. The use of a *C. elegans* Duchenne muscular dystrophy model serves as a prime example of the utility of the nematode for highlighting potential therapeutic agents (33,36,74). In this study, the screening selection criteria were designed to identify and

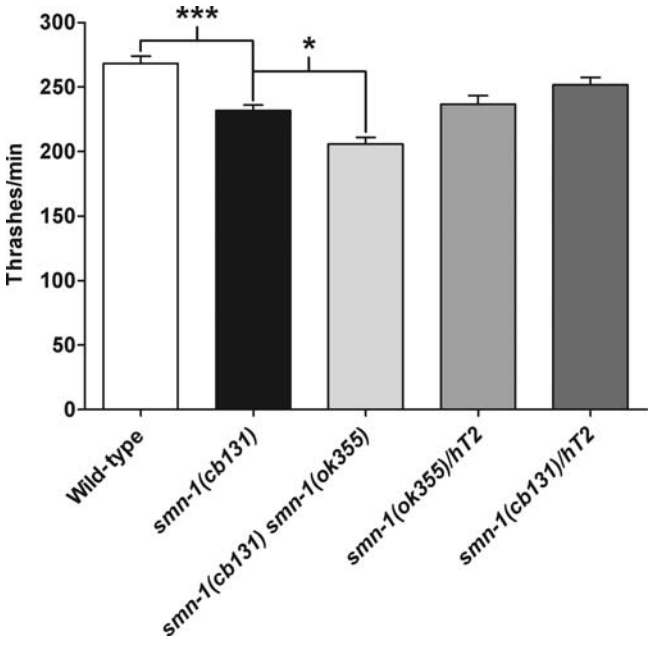

Figure 7. Combining *smn-1(cb131)* and *smn-1(ok355) in trans* does not restore wild-type thrashing rate. *smn-1(cb131)* males were crossed with *smn-1(ok355)/hT2[qIs48]* hermaphrodites and assayed for motility to test for genetic complementation. *smn-1(cb131) smn-1(ok355)* progeny thrashed significantly slower than wild-type, suggesting that the mutations do not complement and are thus both alleles of *smn-1*. *smn-1(cb131)/hT2[qIs48]* animals thrash faster than both *smn-1(ok355)/hT2[qIs48]* and *smn-1(cb131)*, suggesting that *cb131* is not a dominant mutation. Thirty-two animals per strain were assayed over four independent experiments. $P < 0.001$, Kruskal–Wallis test. $^{*}P < 0.05$ and $^{***}P < 0.001$, Dunn's multiple comparison test. Means ± SEM are plotted.

rank candidate compounds with potential for further testing, including the possible future screening of novel analogs based on the structures of the top hits, in the hope of finding a more efficacious compound.

Identification of compounds with potential to treat SMA

Through screening of the NINDS collection of chemical compounds with subsequent validation assays, two FDA-approved drugs—4-AP and gaboxadol hydrochloride—and one novel compound—Neu5Ac—were highlighted that rescued at least one aspect of *smn-1* phenotypic dysfunction and thus may be of interest for further study (Fig. 12). No compound significantly improved the lifespan of the null mutant, but given the extreme nature of the model, this is unsurprising. Importantly for candidate drugs with potential to treat SMA, all three are able to cross the blood–brain barrier (75–77).

4-AP is a dose-dependent potassium channel blocker that can restore conductance along focally demyelinated neurons (78,79) and enhance synaptic transmission by increasing pre-synaptic calcium influx into neurons, prolonging action potential duration (80,81). It therefore has potential for the treatment of neuromuscular disorders and injuries, in which synaptic transmission is affected. Indeed, 4-AP has shown efficacy in models of neurological disease (82,83), and positive results have been obtained in early human trials of 4-AP for the treatment of multiple sclerosis (84–86) and spinal cord injury (87). Here, 4-AP rescued *smn-1(cb131)* motility to wild-type levels (Fig. 10A) and improved growth and neuromuscular function of the null mutant (Fig. 11), making it the most promising candidate from this study. Wild-type thrashing was unaffected, indicating that 4-AP was not simply causing a hyperthrash effect as a result of stress. *unc-63(x26)* motility was also improved by 4-AP, indicating that the positive effect on *cb131* thrashing was not specific to the *smn-1* mutation; however, this does not diminish its potential. Given the action of 4-AP, the conservation of potassium channels in *C. elegans* (88) and that *smn-1(cb131)* displays a synaptic transmission defect, it is unsurprising that 4-AP improved motility of the model. Synaptic transmission is also impaired in *Drosophila* (68) and mouse models of SMA (64,69), which may be a possible cause of muscle weakness in the human disease; 4-AP is therefore an attractive drug for the potential treatment of SMA.

Gaboxadol, or THIP (4,5,6,7-tetrahydroisoxazolo[5,4-c] pyridin-3-ol) as it was previously known, is a potent agonist of a specific extrasynaptic, δ-containing $GABA_A$ receptor subtype, $\alpha_4\beta_3\delta$ (89,90). A late-stage investigational treatment for insomnia, gaboxadol has been shown to activate extrasynaptic receptors in relay neurons of the ventrobasal thalamus (76,91). In *C. elegans*, GABA acts as both an excitatory and inhibitory neurotransmitter (92), making it difficult to suggest a potential mechanism of action in the nematode.

Neu5Ac is a common, negatively charged monosaccharide often found as a terminal component of glycoproteins and glycolipids (gangliosides) on the surface of many animal cells (93). Cleaved from gangliosides by sialidases, it also transiently exists in small quantities in free monomeric form in organs and tissues (94). Interestingly, gangliosides most commonly containing Neu5Ac have been shown to display multiple neurotrophic effects in several neuronal populations, including cholinergic and dopaminergic neurons (95,96). Given the seemingly neuroprotective and neurorestorative properties of gangliosides, they have been explored as potential therapies for neurological disease with reasonable success (97,98); however, the molecular mechanism(s) is not fully known. Recently, a novel function of Neu5Ac as a scavenger of toxic hydrogen peroxide (H_2O_2) was highlighted both in free form and as part of a glycochain (94,99). The ability of Neu5Ac to inhibit cell death caused by H_2O_2 in a dose-dependent manner is hypothesized to be a novel defense mechanism against oxidative damage (94). This suggests a possible mode of action by which Neu5Ac could ameliorate defects associated with *smn-1* dysfunction. *C. elegans* do not possess endogenous sialic acid (100); consequently, any benefit caused by Neu5Ac administration is unlikely to be attributed to increased incorporation into gangliosides. Instead, the enhanced presence of a scavenger of reactive oxygen species may reduce the chances of oxidative damage and thus potential neuronal cell death, which has been implicated in SMA disease progression (101,102).

In summary, we describe a novel *C. elegans smn-1* point mutant that displays various mild phenotypic defects, which is well suited for screening purposes. Using this model, we illustrate the utility of a milder, fertile allele, identifying three candidate compounds with potential for further study in vertebrate models for the treatment of SMA.

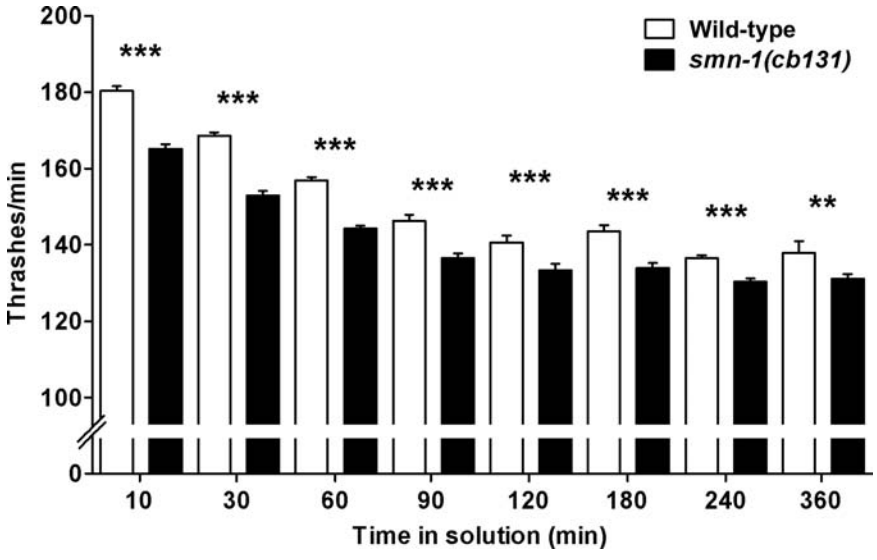

Figure 8. Automated assessment of wild-type and *smn-1(cb131)* thrashing rates. Two days post-L1, a significant difference was seen between wild-type and mutant animals at all time points in PBS. $^{**}P < 0.01$ and $^{***}P < 0.001$, Mann–Whitney *U* test. At least, 69 wells per strain per time point were assayed over three independent experiments. Means ± SEM are plotted.

MATERIALS AND METHODS

Strains and general methods

Strains were maintained under standard conditions on *Escherichia coli* OP50 (48). The following strains were used: N2 Bristol wild-type, NW1229 [*evIs111*[*F25B3.3::GFP; dpy-20(+)*]], LL2058 [*smn-1(cb131) I*], LL2073 [*smn-1(cb131) I*] (4× outcrossed), LM99 [*smn-1(ok355) I/hT2*[*bli-4(e937) let-?(q782) qIs48*] *(I;III)*], LM123 [*smn-1(cb131) I; evIs111*], LM124 [*smn-1(cb131) smn-1(ok355) I*], LM125 [*smn-1(cb131) I/hT2*[*bli-4(e937) let-?(q782) qIs48*] *(I;III)*] and ZZ26 [*unc-63(x26) I*]. All reagents were obtained from Sigma (St Louis, MO) unless otherwise stated.

Isolation of the *smn-1(cb131)* allele

C. elegans bearing the *smn-1* mutant allele *cb131* were isolated from a frozen clonal library of ethyl methane sulfonate-mutagenized animals, as described previously (103). Briefly, the *smn-1* open reading frame (ORF) was amplified by nested PCR from genomic DNA isolated from animals within individual wells of the library. PCR products generated from each library sample were sequenced (using M13 primers), and the data were analyzed using LIMSTILL software (http://limstill.niob.knaw.nl/ last accessed October 19, 2010) to identify missense mutations in *smn-1*. The *smn-1* mutant allele *cb131* was identified using this technique. *cb131* contains a G-to-A mutation at nucleotide 79 of the *smn-1* ORF and is predicted to encode the mutant protein SMN-1 D27N. LL2058 animals homozygous for *cb131* were successfully isolated following resuscitation of the cryopreserved library sample. LL2058 was outcrossed four times to wild-type animals producing LL2073; the presence of the mutant allele was determined by sequencing the *smn-1* locus at each step. Nested primers used to screen for *cb131* were (5′ to 3′): smnF1 catggatatcgtgagactgg; smnF2 tgtaaaacgac ggccagtgcaggcactcatcaaatg, smnR3 aggaaacagctatgaccattcc aacttcgagattatcagc and smnR4 ccgcaatagcttcttcattc; M13 primer sites are underlined.

Body length, development and lifespan assays

For body length measurements, gravid adults were bleached with sodium hypochlorite to obtain embryos, which were then plated at 23.5°C for 48 ± 1 h. Pictures were taken of age-synchronized animals, so that length along the midline from head to tail could be measured using ImageJ software (http://rsb.info.nih.gov/ij/ last accessed October 19, 2010). To assess the rate of development, L4 stage animals were passaged to fresh plates and left at 23.5°C for 24 ± 1 h. Five of the resulting young adults were passaged to a new plate, allowed to lay eggs at 23.5°C for 2 h and then removed. The developmental stage of the progeny was assessed at 24, 48 and 72 h post removal of adults. Over 650 animals per strain per time point were assayed over three independent experiments. Animals were categorized as L1–L2, L3, L4 or young adult based on size and morphological features (104). For lifespan assays, eggs laid by non-starved adults at room temperature (RT) were passaged to *E. coli*-seeded plates and stored at 23.5°C. Survival of individual animals was observed each day at roughly the same time. Animals were scored as dead when unresponsive to prodding of the head and tail with a pick in combination with complete cessation of pharyngeal pumping. Animals were transferred to new plates at least every other day to reduce the chances of contamination.

Egg-laying assays

For characterization of egg-laying behavior, L4 stage animals were transferred to fresh plates and left to mature for 24 ± 1 h at 23.5°C. To quantify the number of eggs laid, young adults

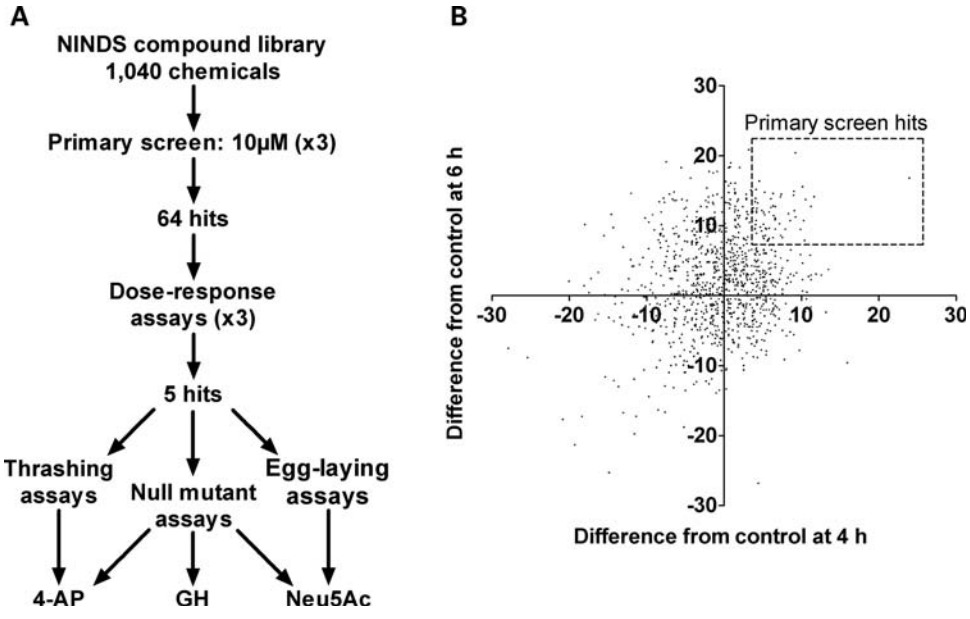

Figure 9. Screening overview and primary screen hits. (**A**) Flow diagram highlighting the screening process. Briefly, the NINDS library comprising 1040 compounds was independently screened three times at 10 μM for amelioration of the *smn-1(cb131)* thrashing defect. This primary screen highlighted 64 compounds, on which dose–response assays were performed subsequently. Six drugs were identified and then assayed for their ability to improve the various defects of *smn-1(cb131)* and the null mutant, *smn-1(ok355)*. 4-AP, 4-aminopyridine; GH, gaboxadol hydrochloride; Neu5Ac, *N*-acetylneuraminic acid. (**B**) Primary screen hit compounds. A scatter graph of the 1040 chemicals showing the median difference in thrashing rate from control at 4 and 6 h (six drugs are outside the lower axis limits). Data represent absolute values.

were singled to individual plates with or without *E. coli*. The number of eggs laid in 2 h at 23.5°C was then counted. Eggs of all shapes, sizes and densities were counted. Mechanical stimulation can inhibit egg-laying, so care was taken not to cause excessive vibration during the assay. To assess the number of eggs retained within the uterus, age-synchronized young adults were transferred to small quantities of 10 mM sodium azide in a 35 mm plate containing multiple thin agar pads. Animals were viewed under a Leica M205 C stereo microscope (Leica, Wetzlar, Germany). For bleaching assays, animals were passaged to individual microtiter wells containing 50 μl 20% sodium hypochlorite solution and left for 5–10 min before counting of dispersed eggs. Thirty animals were assayed per strain over three independent experiments. For brood size assays, L4 stage animals were individually passaged to fresh plates and left at 23.5°C overnight. The following day, the resulting adults were singled to new plates and eggs and hatchlings counted. This was repeated each day until egg-laying ceased. To calculate the percentage of eggs that successfully hatched, 50–100 eggs laid by age-synchronized young adults were transferred to a new plate and then checked the following day to see whether they were still present.

Pharyngeal pumping and swimming (thrashing) and assays

For pharyngeal pumping assays, age-synchronized animals were passaged to freshly seeded plates and left for ≥10 min before assaying. Animals were filmed for 10 s using an XLI 2 Mpixel camera (QImaging, Surrey, BC, Canada) attached to a Nikon SMZ 1000 dissecting microscope (Nikon, Tokyo, Japan) at 12 frames per second, and then videos were played back at a slower rate to allow manual counting of pumps. The number of pumps was multiplied by six to get an estimate per minute. A single pump was scored as a complete backward and forward movement of the terminal bulb grinder. Only animals found within the circumference of food and that were rhythmically and consistently pumping were assayed. For thrashing assays, animals age-synchronized using sodium hypochlorite were picked to individual wells containing 100 μl 1 M PBS and left for 10 min. Every other thrash was counted for 30 s and then multiplied by four to obtain an estimate per minute. A single thrash was defined as a complete change in the direction of the body down the midline. Animals that lingered on well sides or were motionless for ≥10 s were discarded from the analysis.

Muscle and nervous system morphology

To visualize musculature using Nomarski microscopy, young adults age-synchronized by hypochlorite bleaching (2 days post-L1) were mounted in 30 μl M9 on microscope slides and observed using a Zeiss Axioplan 2 microscope with mounted AxioCam (Zeiss, Oberkochen, Germany). For phalloidin staining of F-actin, adapted from Shaham (105), staged young adults were washed off plates into microfuge tubes, frozen in liquid nitrogen and lyophilized using a DNA 120 SpeedVac (Thermo Savant, Holbrook, NY) for 10 min at RT. Two units of Alexa Fluor 488 phalloidin (Invitrogen, Carlsbad, CA) per strain were simultaneously freeze-dried to remove the methanol solvent. An aliquot of 20 μl of ice-cold acetone was then added to the nematodes for 5 min,

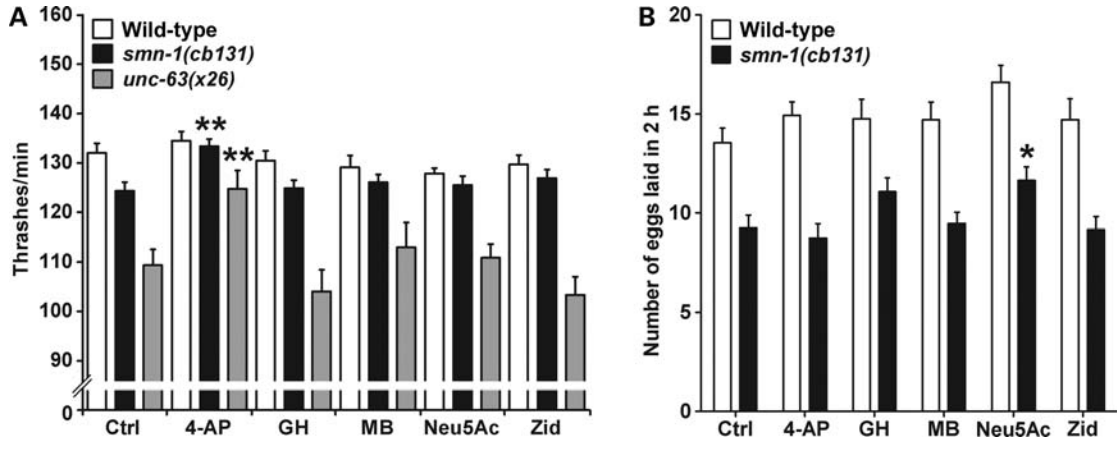

Figure 10. 4-AP rescues *smn-1(cb131)* motility and Neu5Ac improves egg-laying. (**A**) 4-AP significantly rescued thrashing frequency of *smn-1(cb131)* after 1.5, 2, 2.5 and 3 h in solution, did not affect wild-type and improved *unc-63(x26)* thrashing from 1.5 to 2.5 h. Graphs for all four time points were very similar, and only that of 2.5 h is presented. $^{**}P < 0.01$, two-way analysis of variance Bonferroni post-test. About 21–22 wells per strain were assayed for each treatment over four independent experiments. (**B**) Animals were exposed to the top 6 compounds from hatching and the number of eggs laid in 2 h assayed as young adults. None of the compounds had a significant effect on the number of eggs laid by wild-type animals ($P = 0.2523$, Kruskal–Wallis test), whereas Neu5Ac significantly increased (26.1 ± 6.0%) the number of eggs laid by *smn-1(cb131)* compared with PBS control. $P = 0.0112$, Kruskal–Wallis test. $^{*}P < 0.05$, Dunn's multiple comparison test. About 39–40 animals per strain were assayed for each treatment over four independent experiments. Ctrl, control; 4-AP, 4-aminopyridine; GH, gaboxadol hydrochloride; MB, metaraminol bitartrate; Neu5Ac, *N*-acetylneuraminic acid; Zid, zidovudine.

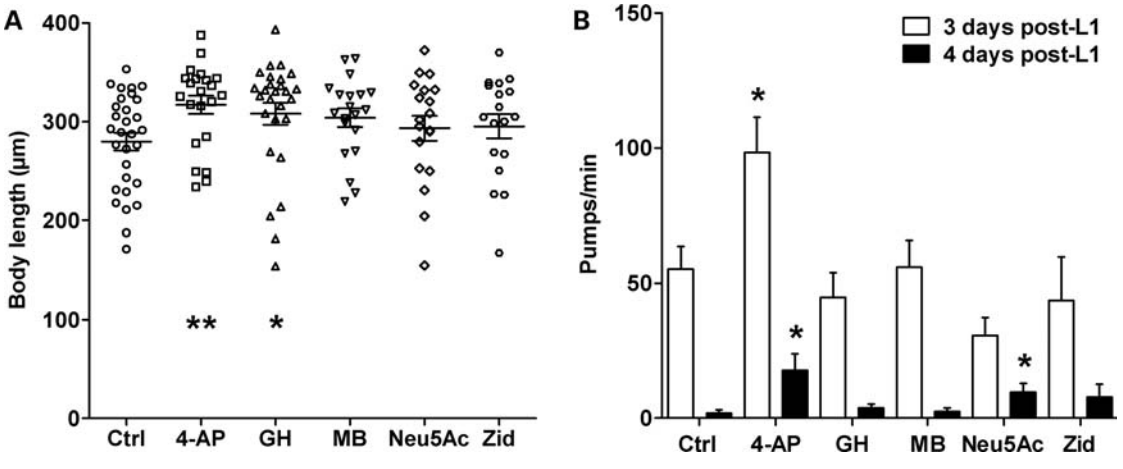

Figure 11. Efficacy of compounds on *smn-1(ok355)*. Null mutant animals were raised on plates containing compounds from hatching and assayed for effects on body length and pharyngeal pumping. (**A**) Three days post-L1, both 4-AP and gaboxadol hydrochloride significantly improved body length. $P = 0.0458$, Kruskal–Wallis test. $^{*}P < 0.05$ and $^{**}P < 0.01$, Dunn's multiple comparison test. About 18–30 animals per treatment were assayed over three independent experiments. (**B**) 4-AP improved pharyngeal pumping rate both 3 and 4 days post-L1, whereas Neu5Ac improved function at 4 days. At 3 days $P = 0.0029$ and 4 days $P = 0.0443$, Kruskal–Wallis test. $^{*}P < 0.05$, Dunn's multiple comparison test. About 15–30 animals were assayed per strain on each day over three independent experiments. Means ± SEM are plotted for both figures. Ctrl, control; 4-AP, 4-aminopyridine; GH, gaboxadol hydrochloride; MB, metaraminol bitartrate; Neu5Ac, *N*-acetylneuraminic acid; Zid, zidovudine.

followed by air drying for 5 min. Meanwhile, 20 µl S-mix (0.2 M sodium phosphate, 0.001 M $MgCl_2$, 0.001% sodium dodecyl sulfate) was mixed with the phalloidin and used to stain F-actin for 30 min at RT. Animals were then washed twice with 0.5% bovine serum albumin and 0.5% Tween-20 in PBS, mounted on microscope slides in a small amount of ProLong Gold antifade reagent (Invitrogen) and visualized using a Zeiss LSM 510 META laser scanning microscope. To perform ventral nerve cord neuron counts and to assess nervous system morphology, age-synchronized young adults were immobilized in 30 µl 10 M levamisole and viewed using a Zeiss Axioplan 2 microscope. Musculature and nervous system morphology were observed independently three times in 10–15 age-synchronized young adults.

Pyridostigmine bromide paralysis assays

L4 stage larvae were passaged to new plates and left for 24 ± 1 h at 23.5°C. Resulting young adults were then transferred to freshly poured plates containing 100 mM pyridostigmine bromide. Drug plates were seeded with 30 µl of bacteria 30–60 min before the assay. Paralysis percentages were calculated by viewing animals at 30 min intervals for 6 h post-plating. Animals were considered paralyzed when

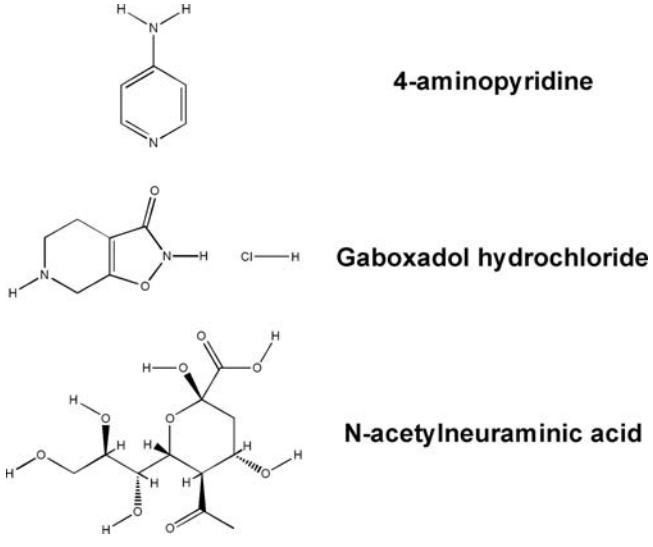

Figure 12. Chemical structures of drugs significantly rescuing the *smn-1* phenotype. The chemical structures of 4-AP, gaboxadol hydrochloride and Neu5Ac are presented. Structures were found at http://pubchem.ncbi.nlm.nih.gov/ (last accessed October 19, 2010).

unresponsive within 5 s to gentle prodding of the head and tail with a pick.

Automated thrashing assays

Animals were age-synchronized by bleaching and placed at 23.5°C for 72 ± 1 h to reach the adult stage. They were then washed into plastic reservoirs with PBS, and 200 µl of this nematode suspension subsequently added to individual wells of a 96-well plate. At various time points in suspension, thrashing rates of animals in individual wells were assessed using an automated phenotyping system (32). For the primary screen, 200 µl PBS containing *smn-1(cb131)* animals was pipetted into individual wells containing 2 µl of drug dissolved in DMSO at a concentration of 1 mM, resulting in a final concentration of 10 µM for each drug. After mixing, animals were left and assayed for thrashing rate after 4 and 6 h. For the dose–response assays, 200 µl PBS containing either *smn-1(cb131)* or wild-type animals was pipetted into wells with the top 64 hits, resulting in concentrations of 50, 25, 12.5, 6.25, 3.13, 1.56 and 0.78 µM in DMSO. For both the primary screen and dose–response assays, the outer two columns of each plate contained 1% DMSO controls.

Screen analysis

For the primary screen, median thrashing rates calculated from the 16 control wells in the outer two columns of each plate were subtracted from the individual thrashing rates to give the difference in thrashing rate compared with the median control value. Median control values were calculated on a plate-by-plate basis in order to reduce the effects of inter-plate variation (the range of plate medians over three trials at 4 and 6 h = 58.9 and 39.0 and SEM = 3.1 and 1.6). The differences in thrashing were calculated at each time point (4 and 6 h) and for each replicate. The median of the three replicates was then taken as the screen score. The arbitrary cut-off criteria, chosen so as to identify approximately the top 5% of compounds, were a difference of greater than or equal to +3.65 thrashes/min at 4 h and greater than or equal to +7.3 at 6 h. For the dose–response assays, dose-dependency curves and non-linear regression coefficients (R^2) were calculated from the raw data ($n = 3$/compound/concentration) generated from three independent experiments. Cut-off criteria for the dose–response assays were a positive trend in the data, $R^2 > 0.1$ and a point along the line of regression ≥7.3 at both 4 and 6 h.

Drug validation assays

Thrashing assays were performed in the same manner as the screen, using optimal concentrations taken from the dose–response assays. For egg-laying experiments, 10–15 L4 stage animals were passaged to new plates with 50 µM compounds and left for 24 ± 1 h at 23.5°C. These plates were freshly seeded with *E. coli* also containing compounds at 50 µM. About 15–20 eggs were then transferred to new drug plates and left for 72 ± 1 h at 23.5°C. These age-synchronized young adults were then assayed for the number of eggs laid in 2 h on plates seeded with 10 µl *E. coli* containing compounds at the same concentration. For the body length, pharyngeal pumping and lifespan assays using *smn-1(ok355)*, 15–20 eggs were passaged to plates containing compounds and left for 72 ± 1 h at 23.5°C. Young adults from these plates were then picked to new drug plates, left for 5 h at 23.5°C to lay eggs and removed. After 48 ± 1 h from first passaging the young adults, progeny not expressing GFP (i.e. homozygous *smn-1* animals) were transferred to new plates and assayed for body length, pumping rate and survival (1 day post-L1). Assays were performed on subsequent days at approximately the same time. Neu5Ac (from bovine milk 98%) used in these assays was purchased from Fisher Scientific (Loughborough, UK).

ACKNOWLEDGEMENTS

The authors thank Dr Kevin Talbot and Professor Kay E. Davies for their encouragement and support of this work, Dr Anne C. Hart for helpful comments on the manuscript, Dr Stuart Grice for help with fluorescence microscopy and the *C. elegans* Gene Knockout Consortium and the *Caenorhabditis* Genetics Center for providing strains. We also acknowledge the generous support of MRCT, including their kind provision of the NINDS library.

Conflict of Interest statement. None declared.

FUNDING

This work was supported by core funding from the Functional Genomics Unit of the Medical Research Council of the UK (J.N.S., S.D.B., B.E. and D.B.S.) and a grant from the Families of SMA (WES0607 to M.V. and B.M.W.). We acknowledge with deep appreciation the generous support to the laboratory received from the family and friends of Jim Murrell.

REFERENCES

1. Pearn, J. (1978) Incidence, prevalence, and gene frequency studies of chronic childhood spinal muscular atrophy. *J. Med. Genet.*, **15**, 409–413.
2. Burghes, A.H. and Beattie, C.E. (2009) Spinal muscular atrophy: why do low levels of survival motor neuron protein make motor neurons sick? *Nat. Rev. Neurosci.*, **10**, 597–609.
3. Lefebvre, S., Burglen, L., Reboullet, S., Clermont, O., Burlet, P., Viollet, L., Benichou, B., Cruaud, C., Millasseau, P., Zeviani, M. *et al.* (1995) Identification and characterization of a spinal muscular atrophy-determining gene. *Cell*, **80**, 155–165.
4. Fischer, U., Liu, Q. and Dreyfuss, G. (1997) The SMN–SIP1 complex has an essential role in spliceosomal snRNP biogenesis. *Cell*, **90**, 1023–1029.
5. Pellizzoni, L., Yong, J. and Dreyfuss, G. (2002) Essential role for the SMN complex in the specificity of snRNP assembly. *Science*, **298**, 1775–1779.
6. Pellizzoni, L., Kataoka, N., Charroux, B. and Dreyfuss, G. (1998) A novel function for SMN, the spinal muscular atrophy disease gene product, in pre-mRNA splicing. *Cell*, **95**, 615–624.
7. Pagliardini, S., Giavazzi, A., Setola, V., Lizier, C., Di Luca, M., DeBiasi, S. and Battaglia, G. (2000) Subcellular localization and axonal transport of the survival motor neuron (SMN) protein in the developing rat spinal cord. *Hum. Mol. Genet.*, **9**, 47–56.
8. Pellizzoni, L., Charroux, B., Rappsilber, J., Mann, M. and Dreyfuss, G. (2001) A functional interaction between the survival motor neuron complex and RNA polymerase II. *J. Cell Biol.*, **152**, 75–85.
9. Pellizzoni, L., Baccon, J., Charroux, B. and Dreyfuss, G. (2001) The survival of motor neurons (SMN) protein interacts with the snoRNP proteins fibrillarin and GAR1. *Curr. Biol.*, **11**, 1079–1088.
10. Lorson, C.L., Hahnen, E., Androphy, E.J. and Wirth, B. (1999) A single nucleotide in the *SMN* gene regulates splicing and is responsible for spinal muscularatrophy. *Proc. Natl Acad. Sci. USA*, **96**, 6307–6311.
11. McAndrew, P.E., Parsons, D.W., Simard, L.R., Rochette, C., Ray, P.N., Mendell, J.R., Prior, T.W. and Burghes, A.H. (1997) Identification of proximal spinal muscular atrophy carriers and patients by analysis of SMN^T and SMN^C gene copy number. *Am. J. Hum. Genet.*, **60**, 1411–1422.
12. Mailman, M.D., Heinz, J.W., Papp, A.C., Snyder, P.J., Sedra, M.S., Wirth, B., Burghes, A.H. and Prior, T.W. (2002) Molecular analysis of spinal muscular atrophy and modification of the phenotype by *SMN2*. *Genet. Med.*, **4**, 20–26.
13. Tzeng, A.C., Cheng, J., Fryczynski, H., Niranjan, V., Stitik, T., Sial, A., Takeuchi, Y., Foye, P., DePrince, M. and Bach, J.R. (2000) A study of thyrotropin-releasing hormone for the treatment of spinal muscular atrophy: a preliminary report. *Am. J. Phys. Med. Rehabil.*, **79**, 435–440.
14. Miller, R.G., Moore, D.H., Dronsky, V., Bradley, W., Barohn, R., Bryan, W., Prior, T.W., Gelinas, D.F., Iannaccone, S., Kissel, J. *et al.* (2001) A placebo-controlled trial of gabapentin in spinal muscular atrophy. *J. Neurol. Sci.*, **191**, 127–131.
15. Kinali, M., Mercuri, E., Main, M., De Biasia, F., Karatza, A., Higgins, R., Banks, L.M., Manzur, A.Y. and Muntoni, F. (2002) Pilot trial of albuterol in spinal muscular atrophy. *Neurology*, **59**, 609–610.
16. Russman, B.S., Iannaccone, S.T. and Samaha, F.J. (2003) A phase 1 trial of riluzole in spinal muscular atrophy. *Arch. Neurol.*, **60**, 1601–1603.
17. Mercuri, E., Bertini, E., Messina, S., Pelliccioni, M., D'Amico, A., Colitto, F., Mirabella, M., Tiziano, F.D., Vitali, T., Angelozzi, C. *et al.* (2004) Pilot trial of phenylbutyrate in spinal muscular atrophy. *Neuromuscul. Disord.*, **14**, 130–135.
18. Weihl, C.C., Connolly, A.M. and Pestronk, A. (2006) Valproate may improve strength and function in patients with type III/IV spinal muscle atrophy. *Neurology*, **67**, 500–501.
19. Liang, W.C., Yuo, C.Y., Chang, J.G., Chen, Y.C., Chang, Y.F., Wang, H.Y., Ju, Y.H., Chiou, S.S. and Jong, Y.J. (2008) The effect of hydroxyurea in spinal muscular atrophy cells and patients. *J. Neurol. Sci.*, **268**, 87–94.
20. Brichta, L., Holker, I., Haug, K., Klockgether, T. and Wirth, B. (2006) *In vivo* activation of *SMN* in spinal muscular atrophy carriers and patients treated with valproate. *Ann. Neurol.*, **59**, 970–975.
21. Mercuri, E., Bertini, E., Messina, S., Solari, A., D'Amico, A., Angelozzi, C., Battini, R., Berardinelli, A., Boffi, P., Bruno, C. *et al.* (2007) Randomized, double-blind, placebo-controlled trial of phenylbutyrate in spinal muscular atrophy. *Neurology*, **68**, 51–55.
22. Tsai, L.K., Yang, C.C., Hwu, W.L. and Li, H. (2007) Valproic acid treatment in six patients with spinal muscular atrophy. *Eur. J. Neurol.*, **14**, e8–e9.
23. Rak, K., Lechner, B.D., Schneider, C., Drexl, H., Sendtner, M. and Jablonka, S. (2009) Valproic acid blocks excitability in SMA type I mouse motor neurons. *Neurobiol. Dis.*, **36**, 477–487.
24. Swoboda, K.J., Scott, C.B., Crawford, T.O., Simard, L.R., Reyna, S.P., Krosschell, K.J., Acsadi, G., Elsheik, B., Schroth, M.K., D'Anjou, G. *et al.* (2010) SMA CARNI-VAL trial part I: double-blind, randomized, placebo-controlled trial of L-carnitine and valproic acid in spinal muscular atrophy. *PLoS ONE*, **5**, e12140.
25. Barber, S.C., Higginbottom, A., Mead, R.J., Barber, S. and Shaw, P.J. (2009) An *in vitro* screening cascade to identify neuroprotective antioxidants in ALS. *Free Radic. Biol. Med.*, **46**, 1127–1138.
26. Desai, U.A., Pallos, J., Ma, A.A., Stockwell, B.R., Thompson, L.M., Marsh, J.L. and Diamond, M.I. (2006) Biologically active molecules that reduce polyglutamine aggregation and toxicity. *Hum. Mol. Genet.*, **15**, 2114–2214.
27. Jarecki, J., Chen, X., Bernardino, A., Coovert, D.D., Whitney, M., Burghes, A., Stack, J. and Pollok, B.A. (2005) Diverse small-molecule modulators of SMN expression found by high-throughput compound screening: early leads towards a therapeutic for spinal muscular atrophy. *Hum. Mol. Genet.*, **14**, 2003–2018.
28. Riessland, M., Ackermann, B., Forster, A., Jakubik, M., Hauke, J., Garbes, L., Fritzsche, I., Mende, Y., Blumcke, I., Hahnen, E. *et al.* (2010) SAHA ameliorates the SMA phenotype in two mouse models for spinal muscular atrophy. *Hum. Mol. Genet.*, **19**, 1492–1506.
29. Westlund, B., Stilwell, G. and Sluder, A. (2004) Invertebrate disease models in neurotherapeutic discovery. *Curr. Opin. Drug Discov. Dev.*, **7**, 169–178.
30. Sleigh, J.N. and Sattelle, D.B. (2010) *C. elegans* models of neuromuscular diseases expedite translational research. *Transl. Neurosci.*, **1**, 214–227.
31. Buckingham, S.D. and Sattelle, D.B. (2008) Strategies for automated analysis of *C. elegans* locomotion. *Invert. Neurosci.*, **8**, 121–131.
32. Buckingham, S.D. and Sattelle, D.B. (2009) Fast, automated measurement of nematode swimming (thrashing) without morphometry. *BMC Neurosci.*, **10**, 84.
33. Gaud, A., Simon, J.M., Witzel, T., Carre-Pierrat, M., Wermuth, C.G. and Segalat, L. (2004) Prednisone reduces muscle degeneration in dystrophin-deficient *Caenorhabditis elegans*. *Neuromuscul. Disord.*, **14**, 365–370.
34. Braungart, E., Gerlach, M., Riederer, P., Baumeister, R. and Hoener, M.C. (2004) *Caenorhabditis elegans* MPP^+ model of Parkinson's disease for high-throughput drug screenings. *Neurodegener. Dis.*, **1**, 175–183.
35. Marvanova, M. and Nichols, C.D. (2007) Identification of neuroprotective compounds of *Caenorhabditis elegans* dopaminergic neurons against 6-OHDA. *J. Mol. Neurosci.*, **31**, 127–137.
36. Giacomotto, J., Pertl, C., Borrel, C., Walter, M.C., Bulst, S., Johnsen, B., Baillie, D.L., Lochmuller, H., Thirion, C. and Segalat, L. (2009) Evaluation of the therapeutic potential of carbonic anhydrase inhibitors in two animal models of dystrophin deficient muscular dystrophy. *Hum. Mol. Genet.*, **18**, 4089–4101.
37. Miguel-Aliaga, I., Culetto, E., Walker, D.S., Baylis, H.A., Sattelle, D.B. and Davies, K.E. (1999) The *Caenorhabditis elegans* orthologue of the human gene responsible for spinal muscular atrophy is a maternal product critical for germline maturation and embryonic viability. *Hum. Mol. Genet.*, **8**, 2133–2143.
38. Burt, E.C., Towers, P.R. and Sattelle, D.B. (2006) *Caenorhabditis elegans* in the study of SMN-interacting proteins: a role for SMI-1, an orthologue of human Gemin2 and the identification of novel components of the SMN complex. *Invert. Neurosci.*, **6**, 145–159.
39. Briese, M., Esmaeili, B., Fraboulet, S., Burt, E.C., Christodoulou, S., Towers, P.R., Davies, K.E. and Sattelle, D.B. (2009) Deletion of *smn-1*, the *Caenorhabditis elegans* ortholog of the spinal muscular atrophy gene, results in locomotor dysfunction and reduced lifespan. *Hum. Mol. Genet.*, **18**, 97–104.
40. Dimitriadi, M., Sleigh, J.N., Walker, A.K., Chang, H.C.-H., Sen, A., Kalloo, G., Harris, J., Barsby, T., Walsh, B., Satterlee, J.S. *et al.* (2010) Conserved genes act as modifiers of invertebrate SMN loss of function defects. *PLoS Genet.*, **6**, e1001172.
41. Sun, Y., Grimmler, M., Schwarzer, V., Schoenen, F., Fischer, U. and Wirth, B. (2005) Molecular and functional analysis of intragenic *SMN1*

mutations in patients with spinal muscular atrophy. *Hum. Mutat.*, **25**, 64–71.
42. Ogawa, C., Usui, K., Aoki, M., Ito, F., Itoh, M., Kai, C., Kanamori-Katayama, M., Hayashizaki, Y. and Suzuki, H. (2007) Gemin2 plays an important role in stabilizing the survival of motor neuron complex. *J. Biol. Chem.*, **282**, 11122–11134.
43. McGovern, M., Yu, L., Kosinski, M., Greenstein, D. and Savage-Dunn, C. (2007) A role for sperm in regulation of egg-laying in the nematode *C. elegans*. *BMC Dev. Biol.*, **7**, 41.
44. Trent, C., Tsuing, N. and Horvitz, H.R. (1983) Egg-laying defective mutants of the nematode *Caenorhabditis elegans*. *Genetics*, **104**, 619–647.
45. Altun-Gultekin, Z., Andachi, Y., Tsalik, E.L., Pilgrim, D., Kohara, Y. and Hobert, O. (2001) A regulatory cascade of three homeobox genes, *ceh-10*, *ttx-3* and *ceh-23*, controls cell fate specification of a defined interneuron class in *C. elegans*. *Development*, **128**, 1951–1969.
46. White, J.G., Southgate, E., Thomson, J.N. and Brenner, S. (1986) The structure of the nervous system of the nematode *Caenorhabditis elegans*. *Phil. Trans. R. Soc. Lond. B. Biol. Sci.*, **314**, 1–340.
47. Argov, Z. (2009) Management of myasthenic conditions: nonimmune issues. *Curr. Opin. Neurol.*, **22**, 493–497.
48. Brenner, S. (1974) The genetics of *Caenorhabditis elegans*. *Genetics*, **77**, 71–94.
49. Piccioni, F., Roman, B.R., Fischbeck, K.H. and Taylor, J.P. (2004) A screen for drugs that protect against the cytotoxicity of polyglutamine-expanded androgen receptor. *Hum. Mol. Genet.*, **13**, 437–446.
50. Abbott, A. (2002) Neurologists strike gold in drug screen effort. *Nature*, **417**, 109.
51. Heemskerk, J., Tobin, A.J. and Bain, L.J. (2002) Teaching old drugs new tricks. Meeting of the Neurodegeneration Drug Screening Consortium, 7–8 April 2002, Washington, DC, USA. *Trends Neurosci.*, **25**, 494–496.
52. Culetto, E., Baylis, H.A., Richmond, J.E., Jones, A.K., Fleming, J.T., Squire, M.D., Lewis, J.A. and Sattelle, D.B. (2004) The *Caenorhabditis elegans unc-63* gene encodes a levamisole-sensitive nicotinic acetylcholine receptor alpha subunit. *J. Biol. Chem.*, **279**, 42476–42483.
53. Sleigh, J.N. (2010) Functional analysis of nematode nicotinic receptors. *Biosci. Horizons*, **3**, 29–39.
54. Kaas, B., Vaidya, A.R., Leatherman, A., Schleidt, S. and Kohn, R.E. (2010) Technical report: exploring the basis of congenital myasthenic syndromes in an undergraduate course, using the model organism, *Caenorhabditis elegans*. *Invert. Neurosci.*, doi: 10.1007/s10158–010–0101–2.
55. Andreassi, C., Jarecki, J., Zhou, J., Coovert, D.D., Monani, U.R., Chen, X., Whitney, M., Pollok, B., Zhang, M., Androphy, E. *et al.* (2001) Aclarubicin treatment restores SMN levels to cells derived from type I spinal muscular atrophy patients. *Hum. Mol. Genet.*, **10**, 2841–2849.
56. Lunn, M.R., Root, D.E., Martino, A.M., Flaherty, S.P., Kelley, B.P., Coovert, D.D., Burghes, A.H., Man, N.T., Morris, G.E., Zhou, J. *et al.* (2004) Indoprofen upregulates the survival motor neuron protein through a cyclooxygenase-independent mechanism. *Chem. Biol.*, **11**, 1489–1493.
57. Andreassi, C., Angelozzi, C., Tiziano, F.D., Vitali, T., De Vincenzi, E., Boninsegna, A., Villanova, M., Bertini, E., Pini, A., Neri, G. *et al.* (2004) Phenylbutyrate increases SMN expression *in vitro*: relevance for treatment of spinal muscular atrophy. *Eur. J. Hum. Genet.*, **12**, 59–65.
58. Brichta, L., Hofmann, Y., Hahnen, E., Siebzehnrubl, F.A., Raschke, H., Blumcke, I., Eyupoglu, I.Y. and Wirth, B. (2003) Valproic acid increases the SMN2 protein level: a well-known drug as a potential therapy for spinal muscular atrophy. *Hum. Mol. Genet.*, **12**, 2481–2489.
59. Pulak, R. (2006) Techniques for analysis, sorting, and dispensing of *C. elegans* on the COPAS flow-sorting system. *Methods Mol. Biol.*, **351**, 275–286.
60. Krause, M., Fire, A., Harrison, S.W., Priess, J. and Weintraub, H. (1990) CeMyoD accumulation defines the body wall muscle cell fate during *C. elegans* embryogenesis. *Cell*, **63**, 907–919.
61. Ardizzi, J.P. and Epstein, H.F. (1987) Immunochemical localization of myosin heavy chain isoforms and paramyosin in developmentally and structurally diverse muscle cell types of the nematode *Caenorhabditis elegans*. *J. Cell Biol.*, **105**, 2763–2770.
62. Avery, L. and Horvitz, H.R. (1989) Pharyngeal pumping continues after laser killing of the pharyngeal nervous system of *C. elegans*. *Neuron*, **3**, 473–485.
63. Murray, L.M., Comley, L.H., Thomson, D., Parkinson, N., Talbot, K. and Gillingwater, T.H. (2008) Selective vulnerability of motor neurons and dissociation of pre- and post-synaptic pathology at the neuromuscular junction in mouse models of spinal muscular atrophy. *Hum. Mol. Genet.*, **17**, 949–962.
64. Ruiz, R., Casanas, J.J., Torres-Benito, L., Cano, R. and Tabares, L. (2010) Altered intracellular Ca^{2+} homeostasis in nerve terminals of severe spinal muscular atrophy mice. *J. Neurosci.*, **30**, 849–857.
65. Dubowitz, V. (1999) Very severe spinal muscular atrophy (SMA type 0): an expanding clinical phenotype. *Eur. J. Paediatr. Neurol.*, **3**, 49–51.
66. Nguyen, M., Alfonso, A., Johnson, C.D. and Rand, J.B. (1995) *Caenorhabditis elegans* mutants resistant to inhibitors of acetylcholinesterase. *Genetics*, **140**, 527–535.
67. Miller, K.G., Alfonso, A., Nguyen, M., Crowell, J.A., Johnson, C.D. and Rand, J.B. (1996) A genetic selection for *Caenorhabditis elegans* synaptic transmission mutants. *Proc. Natl Acad. Sci. USA*, **93**, 12593–12598.
68. Chan, Y.B., Miguel-Aliaga, I., Franks, C., Thomas, N., Trulzsch, B., Sattelle, D.B., Davies, K.E. and van den Heuvel, M. (2003) Neuromuscular defects in a *Drosophila* survival motor neuron gene mutant. *Hum. Mol. Genet.*, **12**, 1367–1376.
69. Kong, L., Wang, X., Choe, D.W., Polley, M., Burnett, B.G., Bosch-Marce, M., Griffin, J.W., Rich, M.M. and Sumner, C.J. (2009) Impaired synaptic vesicle release and immaturity of neuromuscular junctions in spinal muscular atrophy mice. *J. Neurosci.*, **29**, 842–851.
70. Schafer, W.R., Sanchez, B.M. and Kenyon, C.J. (1996) Genes affecting sensitivity to serotonin in *Caenorhabditis elegans*. *Genetics*, **143**, 1219–1230.
71. Loria, P.M., Duke, A., Rand, J.B. and Hobert, O. (2003) Two neuronal, nuclear-localized RNA binding proteins involved in synaptic transmission. *Curr. Biol.*, **13**, 1317–1323.
72. Culetto, E. and Sattelle, D.B. (2000) A role for *Caenorhabditis elegans* in understanding the function and interactions of human disease genes. *Hum. Mol. Genet.*, **9**, 869–877.
73. Harris, T.W., Chen, N., Cunningham, F., Tello-Ruiz, M., Antoshechkin, I., Bastiani, C., Bieri, T., Blasiar, D., Bradnam, K., Chan, J. *et al.* (2004) WormBase: a multi-species resource for nematode biology and genomics. *Nucleic Acids Res.*, **32**, D411–D417.
74. Carre-Pierrat, M., Mariol, M.C., Chambonnier, L., Laugraud, A., Heskia, F., Giacomotto, J. and Segalat, L. (2006) Blocking of striated muscle degeneration by serotonin in *C. elegans*. *J. Muscle Res. Cell Motil.*, **27**, 253–258.
75. Lemeignan, M., Millart, H., Lamiable, D., Molgo, J. and Lechat, P. (1984) Evaluation of 4-aminopyridine and 3,4-diaminopyridine penetrability into cerebrospinal fluid in anesthetized rats. *Brain Res.*, **304**, 166–169.
76. Wafford, K.A. and Ebert, B. (2006) Gaboxadol—a new awakening in sleep. *Curr. Opin. Pharmacol.*, **6**, 30–36.
77. Wang, B., Downing, J.A., Petocz, P., Brand-Miller, J. and Bryden, W.L. (2007) Metabolic fate of intravenously administered *N*-acetylneuraminic acid-6-^{14}C in newborn piglets. *Asia Pac. J. Clin. Nutr.*, **16**, 110–115.
78. Sherratt, R.M., Bostock, H. and Sears, T.A. (1980) Effects of 4-aminopyridine on normal and demyelinated mammalian nerve fibres. *Nature*, **283**, 570–572.
79. Targ, E.F. and Kocsis, J.D. (1985) 4-aminopyridine leads to restoration of conduction in demyelinated rat sciatic nerve. *Brain Res.*, **328**, 358–361.
80. Thesleff, S. (1980) Aminopyridines and synaptic transmission. *Neuroscience*, **5**, 1413–1419.
81. Thomsen, R.H. and Wilson, D.F. (1983) Effects of 4-aminopyridine and 3,4-diaminopyridine on transmitter release at the neuromuscular junction. *J. Pharmacol. Exp. Ther.*, **227**, 260–265.
82. Pinter, M.J., Waldeck, R.F., Cope, T.C. and Cork, L.C. (1997) Effects of 4-aminopyridine on muscle and motor unit force in canine motor neuron disease. *J. Neurosci.*, **17**, 4500–4507.
83. Franciosi, S., Ryu, J.K., Choi, H.B., Radov, L., Kim, S.U. and McLarnon, J.G. (2006) Broad-spectrum effects of 4-aminopyridine to modulate amyloid β_{1-42}-induced cell signaling and functional responses in human microglia. *J. Neurosci.*, **26**, 11652–11664.
84. van Diemen, H.A., Polman, C.H., van Dongen, M.M., Nauta, J.J., Strijers, R.L., van Loenen, A.C., Bertelsmann, F.W. and Koetsier, J.C. (1993) 4-aminopyridine induces functional improvement in multiple sclerosis patients: a neurophysiological study. *J. Neurol. Sci.*, **116**, 220–226.

85. Goodman, A.D., Brown, T.R., Cohen, J.A., Krupp, L.B., Schapiro, R., Schwid, S.R., Cohen, R., Marinucci, L.N. and Blight, A.R. (2008) Dose comparison trial of sustained-release fampridine in multiple sclerosis. *Neurology*, **71**, 1134–1141.
86. Goodman, A.D., Brown, T.R., Krupp, L.B., Schapiro, R.T., Schwid, S.R., Cohen, R., Marinucci, L.N. and Blight, A.R. (2009) Sustained-release oral fampridine in multiple sclerosis: a randomised, double-blind, controlled trial. *Lancet*, **373**, 732–738.
87. Wolfe, D.L., Hayes, K.C., Hsieh, J.T. and Potter, P.J. (2001) Effects of 4-aminopyridine on motor evoked potentials in patients with spinal cord injury: a double-blinded, placebo-controlled crossover trial. *J. Neurotrauma*, **18**, 757–771.
88. Miller, C. (2000) An overview of the potassium channel family. *Genome Biol.*, **1**, REVIEWS0004.
89. Adkins, C.E., Pillai, G.V., Kerby, J., Bonnert, T.P., Haldon, C., McKernan, R.M., Gonzalez, J.E., Oades, K., Whiting, P.J. and Simpson, P.B. (2001) $\alpha_4\beta_3\delta$ GABAA receptors characterized by fluorescence resonance energy transfer-derived measurements of membrane potential. *J. Biol. Chem.*, **276**, 38934–38939.
90. Brown, N., Kerby, J., Bonnert, T.P., Whiting, P.J. and Wafford, K.A. (2002) Pharmacological characterization of a novel cell line expressing human $\alpha_4\beta_3\delta$ GABAA receptors. *Br. J. Pharmacol.*, **136**, 965–974.
91. Jia, F., Pignataro, L., Schofield, C.M., Yue, M., Harrison, N.L. and Goldstein, P.A. (2005) An extrasynaptic GABAA receptor mediates tonic inhibition in thalamic VB neurons. *J. Neurophysiol.*, **94**, 4491–4501.
92. McIntire, S.L., Jorgensen, E., Kaplan, J. and Horvitz, H.R. (1993) The GABAergic nervous system of *Caenorhabditis elegans*. *Nature*, **364**, 337–341.
93. Schauer, R. (2009) Sialic acids as regulators of molecular and cellular interactions. *Curr. Opin. Struct. Biol.*, **19**, 507–514.
94. Iijima, R., Takahashi, H., Namme, R., Ikegami, S. and Yamazaki, M. (2004) Novel biological function of sialic acid (*N*-acetylneuraminic acid) as a hydrogen peroxide scavenger. *FEBS Lett.*, **561**, 163–166.
95. Hadjiconstantinou, M. and Neff, N.H. (1998) GM1 ganglioside: *in vivo* and *in vitro* trophic actions on central neurotransmitter systems. *J. Neurochem.*, **70**, 1335–1345.
96. Mocchetti, I. (2005) Exogenous gangliosides, neuronal plasticity and repair, and the neurotrophins. *Cell. Mol. Life Sci.*, **62**, 2283–2294.
97. Svennerholm, L., Brane, G., Karlsson, I., Lekman, A., Ramstrom, I. and Wikkelso, C. (2002) Alzheimer disease—effect of continuous intracerebroventricular treatment with GM1 ganglioside and a systematic activation programme. *Dement. Geriatr. Cogn. Disord.*, **14**, 128–136.
98. Schneider, J.S., Sendek, S., Daskalakis, C. and Cambi, F. (2010) GM1 ganglioside in Parkinson's disease: results of a five year open study. *J. Neurol. Sci.*, **292**, 45–51.
99. Iijima, R., Takahashi, H., Ikegami, S. and Yamazaki, M. (2007) Characterization of the reaction between sialic acid (*N*-acetylneuraminic acid) and hydrogen peroxide. *Biol. Pharm. Bull.*, **30**, 580–582.
100. Bacic, A., Kahane, I. and Zuckerman, B.M. (1990) *Panagrellus redivivus* and *Caenorhabditis elegans*: evidence for the absence of sialic acids. *Exp. Parasitol.*, **71**, 483–488.
101. Roy, N., Mahadevan, M.S., McLean, M., Shutler, G., Yaraghi, Z., Farahani, R., Baird, S., Besner-Johnston, A., Lefebvre, C., Kang, X. *et al.* (1995) The gene for neuronal apoptosis inhibitory protein is partially deleted in individuals with spinal muscular atrophy. *Cell*, **80**, 167–178.
102. Soler-Botija, C., Ferrer, I., Gich, I., Baiget, M. and Tizzano, E.F. (2002) Neuronal death is enhanced and begins during foetal development in type I spinal muscular atrophy spinal cord. *Brain*, **125**, 1624–1634.
103. Cuppen, E., Gort, E., Hazendonk, E., Mudde, J., van de Belt, J., Nijman, I.J., Guryev, V. and Plasterk, R.H. (2007) Efficient target-selected mutagenesis in *Caenorhabditis elegans*: toward a knockout for every gene. *Genome Res.*, **17**, 649–658.
104. Wood, W.B. (1988) *The Nematode Caenorhabditis elegans*. Cold Spring Harbor Laboratory Press, Cold Spring Harbor, NY, pp. 12–13.
105. Shaham, S. (2006) Methods in Cell Biology (January 02, 2006). In the *C. elegans* research Community (ed.), WormBook. WormBook. doi/10.1895/wormbook.1.49.1, http://www.wormbook.org.